Review Report on "Passive Thermal Stabilization"

Xi Chen

1. Introduction

Athermalization of lens design is always challenging for lens designers. Even though all front-facing mobile phone cameras have VCM auto-focusing, most rear-facing cameras, car cameras and most high-end cameras are fix-focused which are sensitive to temperature change. The IODC2014 conference paper on passive thermal stabilization by Markus Lipp, et. al from Fisba Optik presents a good athermalization design procedure to follow. I will review the optimization with a simple glass substitution method and a paraxial ray-tracing ABCD matrix method described in this paper.

2. Different Methods of Lens Athermalization Optimization

The most straightforward athermalization optimization to do is setting up several configurations in Zemax or CODEV for different temperatures. Then lens designers let the software optimize the thermal performance. But this method is more time consuming and the results could be far away from being optimized depending the starting design which happens a lot for lens design even with global optimization. Alternatively, one could optimize the lens design at nominal temperature only with best combination of optical power distribution between len elements and choices of lens element material. The athermalization is done by calculating the right opto-thermal expansion coefficients (OTEC) of lens elements and replace the elements which are sensitive to temperature with the material with the right OTEC and similar refractive index n_d and similar Abbe number V_d. OTEC is the thermal focus shift coefficient β used in Dr. Burge's class notes. Once the starting design performance is good, lens designers could set up multi-configurations for multiple temperature settings to further fine tune the design for athermalization. The paper describes a way of using paraxial ray tracing (ABCD matrix) of a-ray and b-ray to calculate the image shift due to temperature change for each lens element and air spacing. From this paraxial calculation, one could easily find out which lens surface, thickness and spacing are sensitive to temperature. Optomechanical engineers could improve the athermalization by using special lens barrel material or structure or combination of different metal material to cancel out the focus shift. But this "active" athermalization method is beyond the scope of the paper and this report.

3. Review of the "Passive Thermal Stabilization" Paper

In this section, I will go through the major findings of this paper and my comments on the paper.

3.1 Setting up the optical model

The accurate modeling of the real lens mounts is important to determine the correct air thickness values at different temperatures. Unfortunatelly Zemax makes simple assumption of the lens spacings. In Zemax, the lens elements are mounted by barrel material at the edges of the lenses. The lens center thickness is determined by the edge spacing which is defined by barrel material and the sag change of the lens surface. This simple assumption is not accurate for more complicated mechanical mounting. According to this paper, there are three lens mounting schemes for setting up the thermo-optomechanical model.

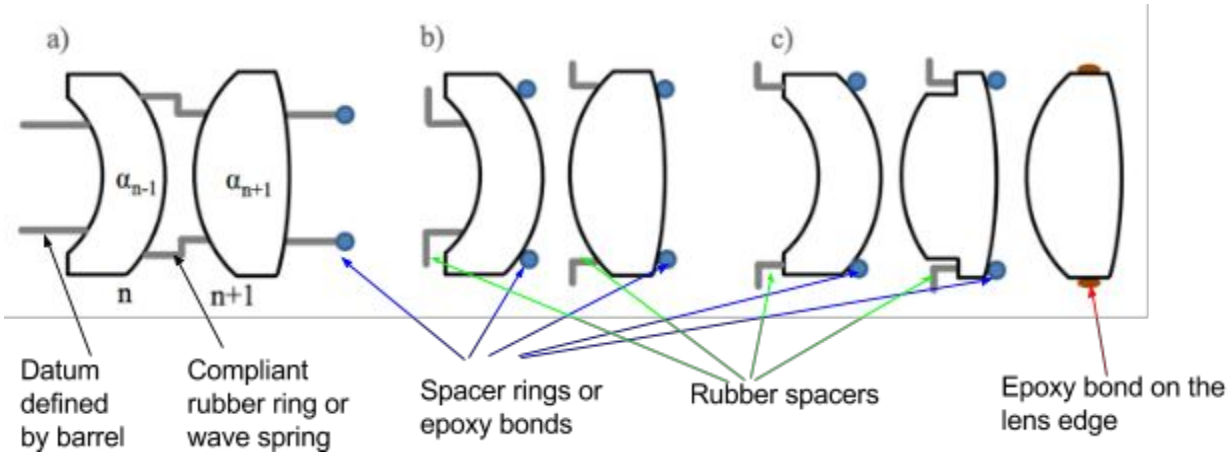

Figure 1 Three lens mounting schemes for setting up the thermo-optomechanical model. (a) rubber tube model; (b) and (c) rubber spacer model.

In (a) rubber tube model, the air spacing between two lens elements is determined by lens stack since there is a compliant rubber ring or wave spring between the two lens elements. The second lens is glued on the rear surface. The first lens sits on the lens barrel housing datum. So the L1S1 and L2S2 surfaces locations need be calculated from barrel structure. L1S2 and L2S1 locations need be calculated from L1S1 and L2S2 locations and lens shape change due to temperature. In (b) and (c) rubber spacer models, the location of each lens' rear surface (bonded and shown in blue dots) could be defined from barrel structure. The front surface location could be calculated with the lens surface shape change due to temperature. The last element in model (c) is bonded from the edge. I think there should be another model for one lens surface sits on a lens barrel datum. Lens designers could write macros to calculate the lens surfaces vertex locations and air thickness for each module and run the macro to set up the thermal optomechanical model in CODEV.

3.2 Thermal analysis

When temperature changes, defocus shows up for fix-focus imaging system and degrades image quality a lot. Nowaday, all front-facing cell phone cameras have VCM (voice coil motor) actuators for autofocusing. But car cameras and most bigger and heavier optical systems are still fix-focused. The author of the paper pointed out that the known quadratic dependency of PV OPD to defocus. The Table 1 below shows the dependency and column 3 of the table shows the dependency of the MTF. To verify Table 1, I derived that the relationship between OPD_{PV} due to defocus and lens Fno is:
$OPD_{PV(defocus)} = \frac{\Delta z'}{8Fno^2}$, where $\Delta z'$ is defocus in image space.

f/#	Defocus until λ/4 PV WFE	Defocus for 5% MTF drop @60lp/mm
20	0.5mm	
10	0.12mm	72µm
5	30µm	24µm
2	4.6µm	7.5µm
1	1.1µm	3.3µm

Table 1 Sensitivity of a perfect, monochromatic, optical system with different Fno depending on the defocus. The target values are $\frac{\lambda}{4}$ PV-OPD and a 5% MTF drop at 60lps/mm.

The defocus can be examined as a function of different parameters of the optical system such as air gaps and the OTEC (β). Even if the optical model is set up with care the thermal analysis has a limited accuracy due to various factors such as the measuring errors of thermal data of the glass and the behavior of bonded joints has to be judged with great care and can lead to an asymmetrical defocus for positive and negative temperatures. Also for the calculation of the thermally induced geometry changes of cemented groups, commercial optical design softwares apply different methods. The author claimed defocus difference in the range of 15µm have been found between the models of the optical software and FEA-results. In the case of optical systems which are very sensitive to temperature changes, the accuracy of simulation can be improved using FEA. In most cases it is possible to adjust the CTE-value of spacer rings, the housing or of the sensor mount to improve thermal performance. The bottom line is we need build good model and find the sensitivity of defocus to temperature and parameters causing worst sensitivity and fix them.

3.3 Thermal Optimization

Two different kinds of thermal optimization methods are described in this subsection. The first one is the glass substitution with sensitivity analysis. I prefer this method as long as there are available glasses with similar refractive index and Abbe # values and quite different OTEC. The second method described in the paper is the paraxial optimization which derives the image shift due to temperature change with only calculation of a-ray and b-ray. To me the second method

is good to find out which lens element and which air thickness is the most sensitive to temperature.

3.3.1 Glass Substitution with Sensitivity Analysis

The sensitivity of the thermal behavior of each lens relating to a certain performance criteria, for instance defocus/ $\Delta OTEC$ can be determined. Alternatively the sensitivity can be estimated for effective focal length change as a function of OTEC (β). The author derived equation for overall lens optical power as a function of lens elements optical powers and equation for the individual lens optical power's change due to temperature. These equations are well-known already. I list them below:

$$\Phi = \sum_{i=1}^{n} \frac{y_{ai}}{y_{a1}} \Phi_i ,$$

where y_{ai} is the a-ray's ray height on lens element i or surface i. Φ_i is the i-th element's optical power and Φ is the image system's optical power.

In Dr. Burge's class, we have learned the focal length and optical power changes due to temperature change which are:

$$\Delta f = f \beta \Delta T \quad \text{and} \quad \Delta \Phi = - \Phi \beta \Delta T,$$

where β is the OTEC (opto-thermal expansion coefficient) of the lens.

With the above two equations, lens designers could easily find out which lens elements are very sensitive to temperature. For example, the lens element with largest $y_a \Phi \beta$ should be most sensitive to temperature.

The author pointed out that most often it is feasible to find substitute glass types with very similar optical properties to the original glass, which allow improving the temperature stability of a lens system with nearly the same nominal optical performance. A very good example for such substitute glasses are the flint glasses in Fig. 2 and Fig. 3. These glasses have very similar optical properties but very different OTEC (see Fig.3). Also other groups of glasses such as the group with Schott N-FK, Ohara S-FPL, Sumita K-PFK glasses including also CaF2 have shown very good substitutional behavior even for broad spectral bands (>500nm) optical systems and although theses glasses have different partial dispersion values. I planned to include a table comparing different glasses' refractive index, Abbe #, partial dispersion values and OTEC for most popular glass catalogs such as Schott, Ohara and Sumita. But due to the very limited time that I have for writing this report, I could not get this nice comparison done here. A good lens designer should have such kind of table handy for glass optimization.

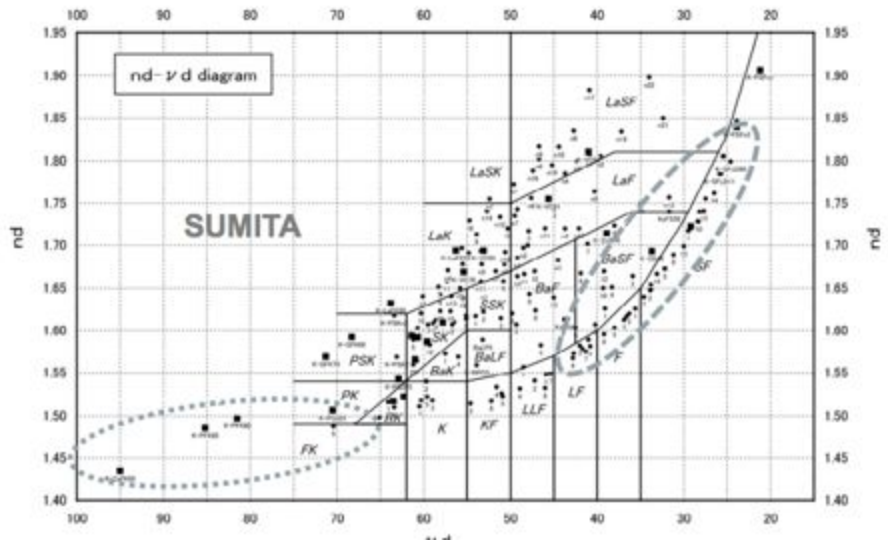

Figure 2 Sumita glass diagram. Two areas with glasses suitable for thermal glass substitution are marked.

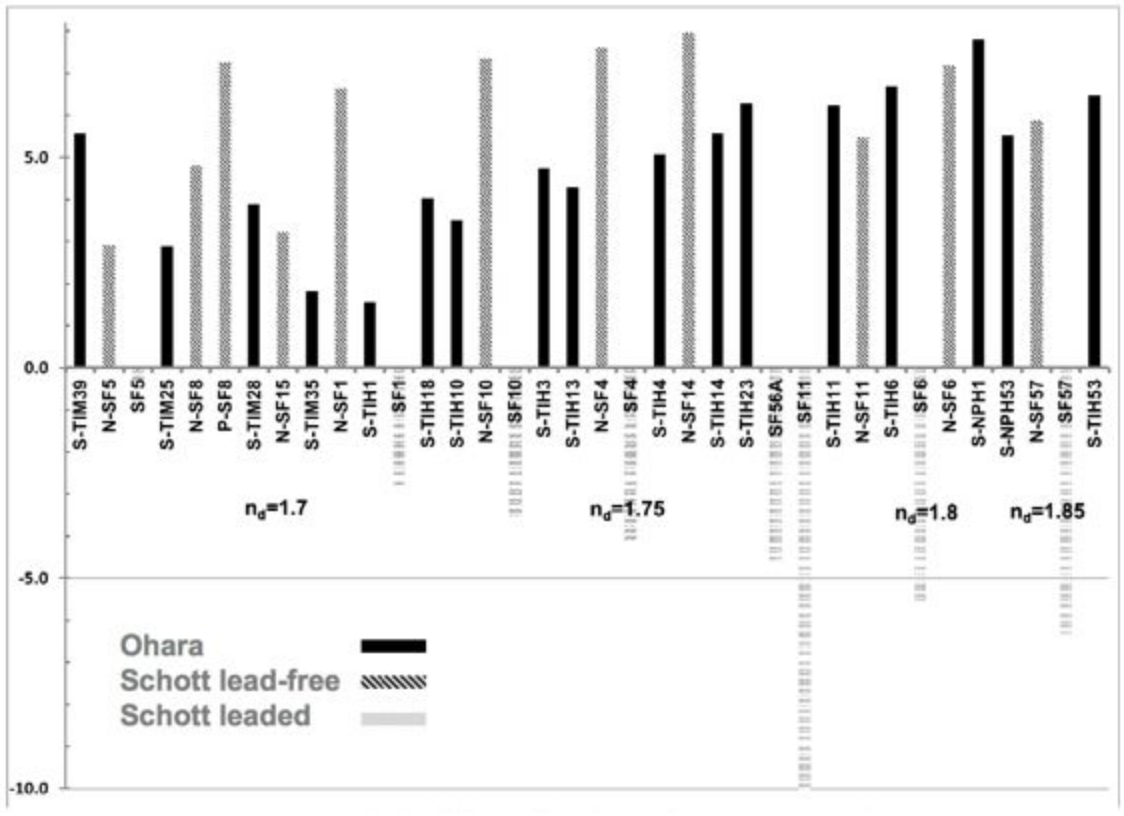

Figure 3 OTEC (n_e, relative) for different flint glasses from Schott and Ohara.

3.3.2 Paraxial Optimization

In this subsection, the author derived how to calculate image shift on the fixed image plane from simple a-ray and b-ray ray heights and angles at nominal temperature. Details of derivation will not shown here. Anyone interested in the derivation could find more details in Appendix.
The image transverse (lateral) shift on the fixed image plane due to the distance change of δ between two surfaces i and i+1 due to the temperature change is:

$$\frac{-\delta u_{ai}^2 y_b}{y_{a,i+1}u_{bi}-y_{b,i+1}u_{ai}} = \frac{-\delta NA_i^2 y_b}{y_{a,i+1}u_{bi}-y_{b,i+1}u_{ai}},$$

where $y_{a,i}$ and $u_{a,i}$ are the a-ray's (marginal ray) ray height and ray slope with respect to the optical axis. Similarly $y_{b,i}$ and $u_{b,i}$ are the b-ray's (chief ray) ray height and ray slope with respect to the optical axis. The denominator in the equation above is similar to the Lagrange's Invariant if i+1 is replaced by i. Unfortunatelly it is not the Lagrange's Invariant. One could easily obtain the defocus amount due to distance change caused by temperature change from the equation above which is

$$defocus = \frac{-\delta NA_i^2 y_b}{NA(y_{a,i+1}u_{bi}-y_{b,i+1}u_{ai})}.$$

When distance change δ is the air spacing change, this change leads to lens shift ΔZ_L. Dr. Burge published a paper on how to calculate defocus due to lens element axial shift. The defocus on image plane ΔZ is:

$$\Delta Z = \Delta Z_L \frac{NA_{i+1}^2 - NA_i^2}{NA^2}.$$

Comparing the defocus change due to thickness or air spacing changes given in the paper and the well-known defocus change due to lens element axial shift given by Dr. Burge, I could not draw a conclusion that they agree with each other. From insight, it is hard for me to imagine why defocus depends on chief-ray height too. Unfortunatelly I wrote this report in a big hurry, I did not have enough time to verify all equations derived in this passive athermalization paper. Separately, temperature changes also influence the lens radii R and refractive indices n. Thereby the slope of the marginal ray is changed. The resulting error in the image plane due to lens radii and refractive indices change is:

$defocus = \tau \frac{y_{ai} y_b}{NA * H}$,

Where $\tau = -\alpha \frac{y_{ai}}{R_i}(\frac{n_{i-1}}{n_i} - 1)$ for change in radius R_i and $\tau = \frac{\partial}{\partial T}(\frac{n_{i-1}}{n_i})(u_{ai} + \frac{y_{ai}}{R_i})$.

The defocus dependence on thickness or spacing changes and lens radii and refractive indices changes is very useful for lens designer to specify the tolerance budgets for the thermal performance and fix the sensitive parameters.

4. Summary

The reviewed paper made an example of a thermally stabilized optical system (EFL of 30mm, f/1.3, 450nm-1000nm) with rubber spacer model. The athermalization was achieved using the prescribed glass substitution method in combination with housing modifications and a subsequent multi-configuration optimization. The measured MTF data are in good compliance

with the design simulation. For the thermal stabilization of temperature-sensitive optical systems, it is necessary to use a precise optical model that account for real lens mounts instead of using the simple barrel “dominant” model in Zemax. For analysis slightly different calculation methods of the available optical design software have to be taken into account. I should carefully compare the difference in opto-thermal models between Zemax and CODEV in near future. Especially the simulation of the thermal behavior of cemented components can deviate from calculations using FEA. To account for the limited accuracy of the thermal analysis it is recommended to allow for compensation. For the improvement of the thermal stability of the system, a lens material substitution method and a paraxial method for finding out the sensitivity of different lens parameters to temperature have produced very good results. For balancing of the optical performance these methods combining with multiple-configuration optimization.

5. References

[1] ZEMAX User’s Manual.
[2] Markus Lipp, et al., “Passive Thermal Stabilization,” SPIE Vol. 9293, 929323-1 to 929323-7 (2014).
[3] Katie Schwertz and J. H. Burge, “Relating Axial Motion of Optical Elements to Focal Shift,” Proc. of SPIE Vol. 7793, 779306-1 to 779306-14 (2010).
[4] W. J. Smith, *Modern Lens Design*, *2nd Edition*, (McGraw-Hill, 2005).

6. Appendix

The derivations of the paraxial optimization equations in the paper are shown here. Note: all symbols are exactly the same as the symbols used in the original paper.
On every surface the ray heights of the paraxial chief ray and the marginal ray (r, s) and the slopes after each surface (s, v) are calculated:

$$\boldsymbol{M} = \begin{pmatrix} r \\ u \end{pmatrix} \quad \boldsymbol{C} = \begin{pmatrix} s \\ v \end{pmatrix}$$

Due to linearity of paraxial optics, every paraxial ray can be described as a linear combination x·M+y·C of these two rays. If the distance between two surfaces i and i+1 is changed with δ the ray height of the marginal ray is also changed. The new marginal ray can be described as a linear combination of the original rays M and C:

$$\mathbf{M} = \begin{pmatrix} r_{i+1} \\ u_i \end{pmatrix} \rightarrow \begin{pmatrix} r_{i+1} + u_i \cdot \delta \\ u_i \end{pmatrix} = (1+a) \cdot \boldsymbol{M} + b \cdot \boldsymbol{C}$$

The height of the new ray in the focus plane is a measure for the defocus and is

$$(1+a) \cdot r_{img} + b \cdot s_{img} = b \cdot s_{img} \quad (with\ r_{img} = 0)$$

The above system of equations results in

$$b = \frac{-\delta \cdot u_i^2}{r_{i+1} \cdot v_i - s_{i+1} \cdot u_i}$$

Temperature changes also influence the lens radii R and the refractive indices n. Thereby the slope of the marginal ray is changed with $\tau = \tau_\alpha + \tau_n$. (α: radius, n: refractive index).

$$\tau_a = -\alpha \cdot \frac{r_i}{R_i} \cdot \left(\frac{n_{i-1}}{n_i} - 1\right)$$

$$\tau_n = \frac{\partial}{\partial T}\left(\frac{n_{i-1}}{n_i}\right) \cdot \left(u_i + \frac{r_i}{R_i}\right)$$

Again the new marginal ray is a combination of the original rays:

$$\mathbf{M} = \begin{pmatrix} r_i \\ u_i \end{pmatrix} \rightarrow \begin{pmatrix} r_i \\ u_i + \tau \end{pmatrix} = (1 + a') \cdot \boldsymbol{M} + b' \cdot \boldsymbol{C}$$

Here the solution of the equations is

$$b' = \frac{\tau \cdot r_i}{r_i \cdot v_i - s_i \cdot u_i}$$

The resulting error in the image plane is $b' * S_{img}$. Because all errors are small, the total system error can be calculated as sum of the individual errors.